Physical principles underlying the transduction of bilayer deformation forces during mechanosensitive channel gating

Eduardo Perozo[1], Anna Kloda[2], D. Marien Cortes[1] and Boris Martinac[2]

Published online: 12 August 2002, doi:10.1038/nsb827

In mechanosensitive (MS) channels, gating is initiated by changes in intra-bilayer pressure profiles originating from bilayer deformation. Here we evaluated two physical mechanisms as triggers of MS channel gating: the energetic cost of protein–bilayer hydrophobic mismatches and the geometric consequences of bilayer intrinsic curvature. Structural changes in the *Escherichia coli* large MS channel (*MscL*) were studied under nominally zero transbilayer pressures using both patch clamp and EPR spectroscopic approaches. Changes in membrane intrinsic curvature induced by the external addition of lysophosphatidylcholine (LPC) generated massive spectroscopic changes in the narrow constriction that forms the channel 'gate', trapping the channel in the fully open state. Hydrophobic mismatch alone was unable to open the channel, but decreasing bilayer thickness lowered MscL activation energy, stabilizing a structurally distinct closed channel intermediate. We propose that the mechanism of mechanotransduction in MS channels is defined by both local and global asymmetries in the transbilayer pressure profile at the lipid–protein interface.

Mechanosensitive (MS) channels fulfill a major role in the responses of living organisms to mechanical stimuli by catalyzing the transfer of ions and other solutes across the membrane in response to changes in bilayer tension. These channels function as mechanoelectrical switches in such diverse physiological processes as touch, hearing, proprioception, turgor control in plant cells and osmoregulation in bacteria[1–6]. The best studied of these MS channels is the large conductance channel from *Escherichia coli* (MscL), first identified, purified and cloned by Kung and collaborators[7,8] through classical membrane fractionation methods and *in vitro* testing of channel activity. The structure of MscL in the closed state reveals a homo pentamer with two transmembrane (TM) segments per subunit[9]. All TM1 segments associate near the five-fold axis of symmetry to form a narrow constriction (2 Å wide) lined by hydrophobic residues that physically restrict ion flow. Patch-clamp experiments have shown that MscL gates in response to an increase in transbilayer pressure, generating a large pressure-activated, nonselective conductance of ~3 nS (Fig. 1*a*)[8,10]. In spite of the thorough functional and structural analysis carried out thus far on MscL channels, the mechanism of mechanical energy transduction from bilayer deformation to protein movement is still not understood. Nonetheless, membrane deformation (either in the form of an osmotic downshock or as negative pressure applied from a patch-clamp pipette) must generate significant changes in the bilayer lateral pressure profile[11,12] (Fig. 1*b*) to ultimately trigger channel opening.

The observation that *MscL* can be activated by pressure gradients after reconstitution in pure lipid systems[8] indicates that this channel is gated by tension transmitted through the bilayer alone. Thus, protein–lipid interactions must play a fundamental role in defining the physical principles that underlie MscL gating. There are numerous examples in the literature[13–16] establishing the importance of the bilayer mechanical properties, such as the extent of hydrophobic mismatch or the intrinsic curvature of a leaflet, in determining membrane protein function. The functional consequences of hydrophobic mismatch are mostly due to the energetic cost of either exposing hydrophobic groups to the high dielectric of water or to the burial of polar groups into the lipid environment[16–20]. Hydrophobic mismatch can be controlled experimentally by using phospholipids with different acyl chain lengths[21] that either compress or expand the lateral pressure profile (Fig. 1*b*). An increase in bilayer curvature, in contrast, tends to produce shifts in the pressure-dependence of the open probability curve toward smaller pressures (Fig. 1*b*), favoring the open state. Intrinsic curvature can be easily changed through the use of lipid mixtures[22]. Indeed, electrophysiological evidence suggests that in MS channels open probability (P_O) can be modulated *in vitro* by the addition of cone-shaped molecules (charged amphipaths, certain anesthetics or lysophospholipids)[23–26]. However, this simple interpretation of lipid shape effects is further complicated because the addition of lysophospholipids generates changes in both intrinsic curvature and membrane thickness[27]. Consequently, the question remains open as to whether the physical basis of the transduction events in mechanosensitive channels can be explained by hydrophobic mismatch, intrinsic curvature or a combination of both effects.

Here we directly address this question by combining single channel recordings and electron paramagnetic resonance (EPR) spectroscopic measurements of MscL reconstituted in a variety of lipid environments. EPR spectroscopy, in combination with site-directed spin labeling (SDSL), has become a powerful technique in the analysis of membrane protein structure and conformation[28–30]. Using this approach, EPR analysis of lipid-reconstituted

[1]Department of Molecular Physiology and Biological Physics, University of Virginia, Charlottesville, Virginia 22906, USA. [2]Department of Pharmacology, Queen Elisabeth II Medical Center, University of Western Australia, Crawley, Western Australia 6009, Australia.

Correspondence should be addressed to E.P. *email: eperozo@virginia.edu*

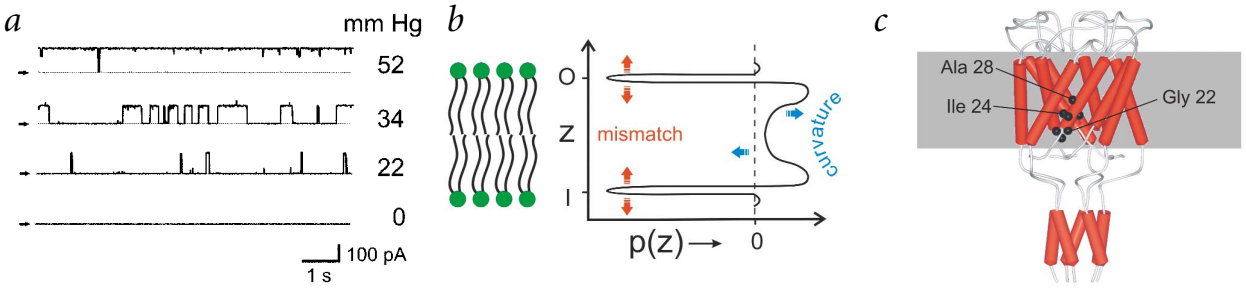

Fig. 1 MscL gating is triggered by transbilayer pressure gradients and transduced *via* intra-bilayer tension changes. ***a***, The single channel activity from purified and reconstituted MscL depends sharply on transmembrane pressure differences. The patch-clamp experiment is carried out on giant asolectin liposomes at pH 7.2 (scale bars correspond to 1 s and 100 pA). This recording was obtained at a holding potential of +30 mV by applying negative pressure to the patch pipette. ***b***, Transbilayer lateral pressure profile p(z). The y-axis corresponds to the membrane depth (z) from the intracellular leaflet (I) to the extracellular one (O). The relative dimensions of a bilayer are represented by the schematic diagram on the left. Data are re-plotted from previous results[11,12]. ***c***, MscL residue positions subjected to site-directed spin labeling (black spheres). The three-dimensional structure[9] is shown with its secondary structure elements represented as cylinders.

MscL[31] revealed that the crystal structure of MscL[9] is actually a good representation of the channel structure in its native environment even though it was determined in detergent micelles. In the present study, we have focused on the narrowest segment along the MscL permeation pathway (the N-terminal half of the first transmembrane segment, TM1) as an ideal region to monitor gating related structural rearrangements in MscL[32]. To this end, all patch-clamp experiments were performed on wild type MscL, and EPR experiments were done on MscL Cys mutants that were spin labeled at positions 20–28 (Fig. 1*c*). In each case, data were obtained under conditions that modify either (i) hydrophobic bilayer matching or (ii) the internal bilayer profile through curvature changes. Given the size of the gating-related conformational changes in MscL, populating the open state for the chosen mutant set is expected to be characterized by a large increase in probe motility together with a complete elimination of any intersubunit spin–spin interactions.

Influence of hydrophobic mismatch

To evaluate the functional consequences of bilayer hydrophobic mismatch, we first carried out patch-clamp experiments on MscL reconstituted in lipids with different acyl chain lengths. Wild type MscL was reconstituted in synthetic phosphatidylcholine (PC) containing monosaturated chains of 14, 16, 18 (control), 20 and

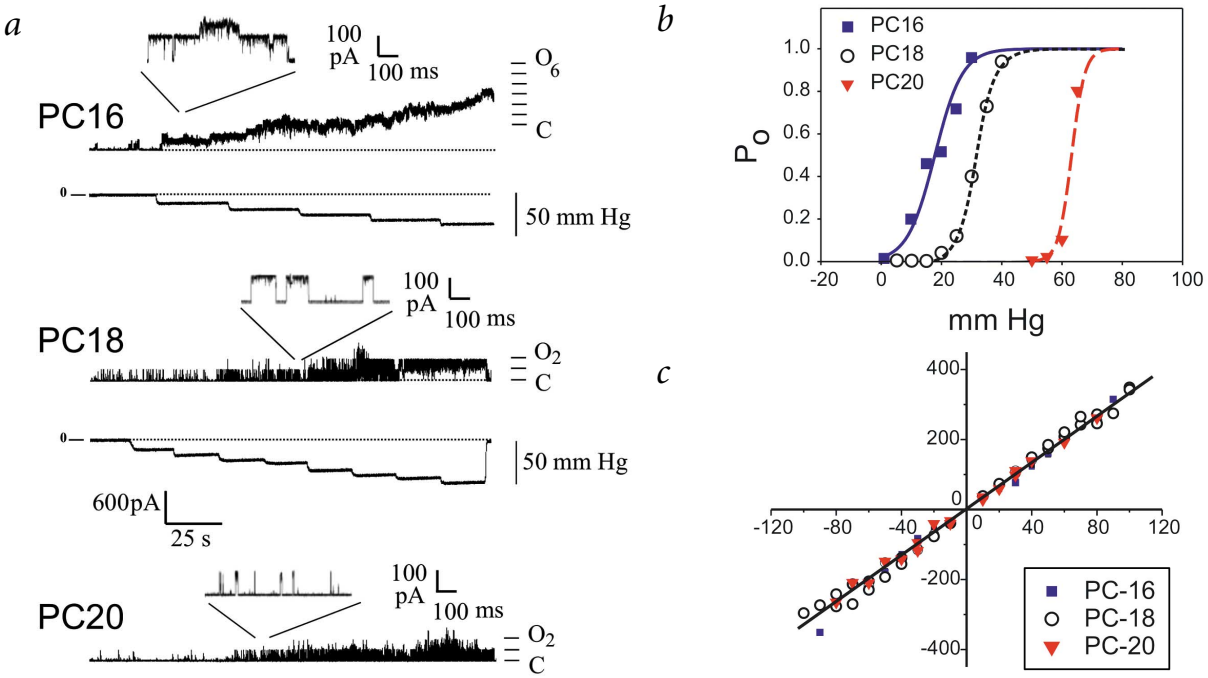

Fig. 2 Hydrophobic surface matching stabilizes intermediate conformations but does not fully open MscL. ***a***, Representative single channel current traces of MscL reconstituted in phosphatidylcholines of different acyl chain lengths. Traces show (sequentially from the top) data obtained in 16:1 dipalmitoleoyl-phosphatidylcholine (PC16), 18:1 dioleoyl-phosphatidylcholine (PC18, taken as the control length) and 20:1 Eicosenoyl-phosphatidylcholine (PC20). Data were obtained at room temperature, holding the membrane at +30 mV and at pH 7.2. ***b***, Pressure dependence of MscL is shifted in the pressure axis. Gating curves represent Boltzmann distribution fits to the data of the form $P_O = P_{max} / (1 + \exp \alpha (P_{1/2} - P))$, where P_O and P_{max} are the open and maximal open probabilities; P; the applied transmembrane pressure (in mm Hg); P_Ω, the pressure at which the channels are open half the time ($P_O = 0.5$); and α, the slope factor. Fits were obtained with the following parameters: PC16, $P_{1/2}$ = 25.6 mm Hg and α = 0.16 mm Hg^{-1}; PC18, $P_{1/2}$ = 45 mm Hg and α = 0.20 mm Hg^{-1}; and PC20, $P_{1/2}$ = 73.4 mm Hg and α = 0.35 mm Hg^{-1}. ***c***, Current to voltage relationship for MscL under the same conditions above.

22 carbons. Because of a sharp increase in liposome fragility, we were unable to obtain complete data sets for MscL reconstituted in bilayers PC14 or shorter, whereas PC22 bilayers inhibited channel reconstitution. Nevertheless, the data in PC20, PC18 and PC16 firmly established significant effects of bilayer mismatch on MscL gating properties. Compared to the recording in PC18 (control), MscL opens with a significantly lower activation threshold in PC16 bilayers while simultaneously requiring lower pipette pressures to fully open. The opposite behavior is observed for MscL reconstituted in PC20 bilayers (Fig. 2*a*). Thus, thin bilayers favor channel openings, whereas thick bilayers tend to stabilize the closed configuration. This is the expected result if TM segments in the open state were considerably tilted towards the plane of the bilayer[33–35]. Complete P_O *versus* pressure curves also demonstrate that the extent of hydrophobic mismatch does not seem to affect the pressure dependence of channel opening (Fig. 2*b*). Rather, mismatch seems to exert a constant pressure bias that simply shifts the midpoint of the open probability curve to higher or lower pressures, depending on the nature of the mismatch, generating destabilization energies as large as 13 kT (Table 1). These energies are in a good agreement with the energies calculated for the improved MscL–bilayer match assuming a stretch-induced bilayer thinning of ~1 Å (ref. 4). Nevertheless, they are a few kT less than the experimentally determined energy of 18.6 kT required to fully open MscL[36], which indicates that the membrane area occupied by MscL is approximately constant in lipids of different thickness in our experiments. These shifts in the apparent $P_{1/2}$ value occur without noticeable changes in the single channel conductance (Fig. 2*c*; Table 1).

Table 1 Functional properties of MscL channels as a function of hydrophobic mismatch

Lipid	α (mm Hg^{-1})[1,2]	$P_{1/2}$ (mm Hg)[1,3]	ΔG_o (kT)[1,4]	n	g (nS)[1]
PC16	0.19 ± 0.04	24.0 ± 2.3	4.0 ± 0.2	7	3.4 ± 0.1 (n = 3)
PC18	0.26 ± 0.04	42.0 ± 4.6	9.4 ± 0.7	10	3.4 ± 0.1 (n = 3)
PC20	0.36 ± 0.06	72.7 ± 7.7	23.5 ± 1.5	9	3.5 (n = 2)

[1]Number is the mean ± S.E.
[2]α = pressure sensitivity (1 / α is the amount of negative pressure in mmHg required for e-fold change in the channel open probability).
[3]$P_{1/2}$ = pressure required for the channel open probability; P_O = 0.5.
[4]ΔG_o, It can be shown that the free energy difference between the closed and open channel in the absence of membrane tension is given by the product of α and $P_{1/2}$ — that is $\Delta G_O / kT = \alpha \times P_{1/2}$ (ref. 4). It is the energy required to open the channel. Where $\alpha = r\Delta A / 2kT$ and $P_{1/2} = 2\Delta G_O / r\Delta A$ (r = radius of curvature in of the patch, ΔA = difference in membrane area occupied by open and closed channel); g is single channel conductance and n indicates the number of experiments carried out under the same experimental conditions. One way analysis of variance (ANOVA) gave $P < 0.001$ significance for the pairwise multiple comparison of the values of ΔG_O for the three lipids. The differences in the mean values of α are not statistically great enough ($P = 0.293$) to exclude the possibility that the difference is due to random sampling variability.

Although we could not reliably impose pressure gradients on bilayers formed by lipids shorter than 14 carbons, we were able to test the effects of a wider range of phospholipid lengths by monitoring EPR lineshape changes in residues at the start of TM1 (positions 20–28, Fig. 1*c*) in the absence of transbilayer pressures. In addition to PC20, PC18 and PC16, each spin-labeled mutant was reconstituted into liposomes made of phosphatidylcholine with even shorter acyl chain lengths: PC14, PC12 and PC10 (PC10 is the shortest phospholipid able to form bilayers). Spectra for residues Gly 22, Ile 24, Ile 25 and Ala 28 represent different sides of the TM1 helix (color coded for the particular phospholipid length used during reconstitution, Fig. 3*a*). We monitored the structural changes by following the variations in EPR spectral lineshape corresponding to probe dynamics (ΔH_O) and spin–spin interactions (Ω), an indication

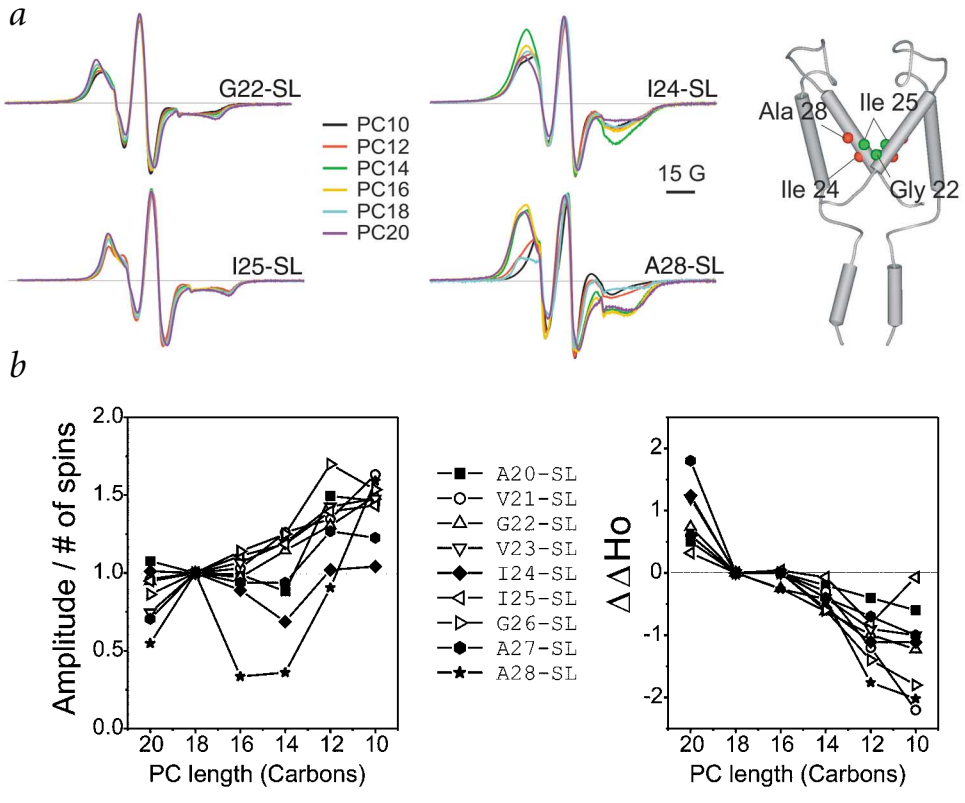

Fig. 3 Hydrophobic mismatch induces conformational rearrangements of MscL gate. ***a***, CW-EPR spectra for selected spin-labeled MscL reconstituted in the following lipids: PC20, PC18, PC16, 14:1 dimirstoyl-phosphatidylcholine (PC14), 12:0 dilauroyl-phosphatidylcholine (PC12) and 10:0 dicaproyl-phosphatidylcholine (PC10). Spectra were obtained with a 150 G scan at room temperature. The right panel shows the location of the selected residues in the closed state MscL structure. ***b***, Relative changes in spin-label motional freedom ($\Delta\Delta H_O$) and estimated intersubunit proximity (Ω) as a function of acyl chain length. Data were normalized in relation to PC18. The chosen stretch of 9 consecutive residues (20–28) constitutes the narrowest segment of MscL permeation pathway.

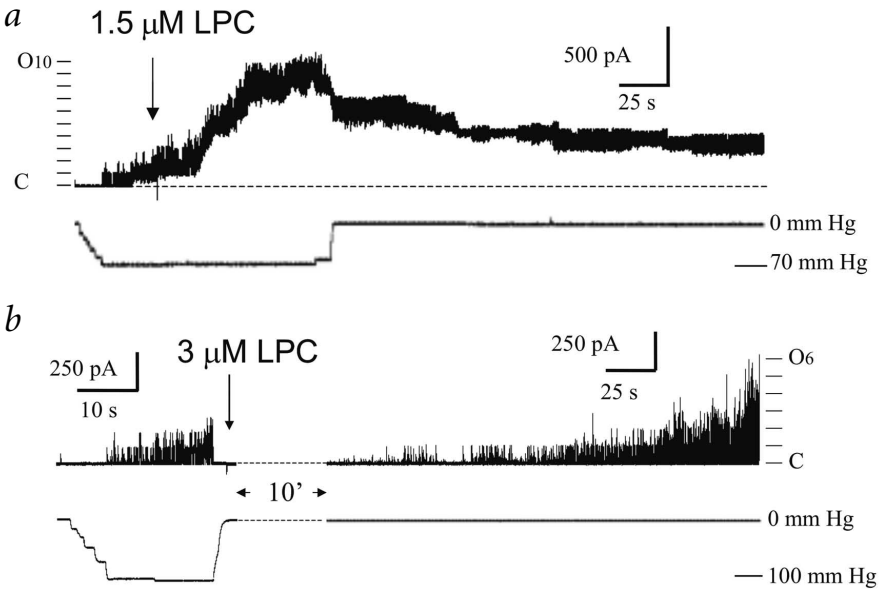

Fig. 4 Stabilization of open MscL with mixtures of PC–LPC. The activation of MscL was measured in the presence of LPC applied to the external solution either ***a***, during slight negative transbilayer pressure (1.5 μM) or ***b***, in the absence of applied pressure (3 μM). Pipette voltage was +30 mV.

of subunit proximity. Positions Gly 22 and Ile 25 show some lineshape changes, with small increases in probe mobility but limited changes in broadening resulting from spin–spin coupling. However, even in the shortest bilayer (PC10), these spectral changes are far subtler than those expected for a transition leading to a fully open state. More interesting, although positions Ile 24 and Ala 28 reveal significant lineshape changes, they display increased spin coupling spectral broadenings at intermediate membrane thickness (PC16 and PC14), as if this region of TM1 moved nearer to the symmetry axis, further narrowing the extracellular aqueous vestibule present in the closed state. Mismatches resulting from MscL incorporation into thicker bilayers (PC20) resulted in significant reductions in probe mobility at all measured positions (Fig. 3*a*), with small changes in spin coupling for residues Val 23, Gly 26, Ala 27 and Ala 28. This finding is in agreement with the idea that thicker bilayers drive the channel deeper into the closed state.

An analysis of the changes in spin–spin coupling (Ω) and probe mobility ($\Delta\Delta H_O$) as a function of lipid length (Fig. 3*b*) indicates that both of these parameters point to a global mismatch-driven conformational change of MscL in which residues 20–28 become, on average, less motionally restricted while, in some cases (open symbols), monotonically increasing their intersubunit separation. However, the behavior of Ala 20, Ile 24, Ala 27 and Ala 28 (filled symbols) strongly suggest that these conformational changes do not correspond to the fully open state. The dependence of the Ω parameter with lipid chain length shows an interesting biphasic behavior: in the range between PC20 and PC14, the magnitude of spin coupling increases (lower Ω), suggesting that these residues become closer to each other and to the axis of symmetry. Further reductions in bilayer thickness (between PC 14 and PC10) promote a significant decrease in the magnitude of the spin–spin coupling (residues move away from each other). In one case

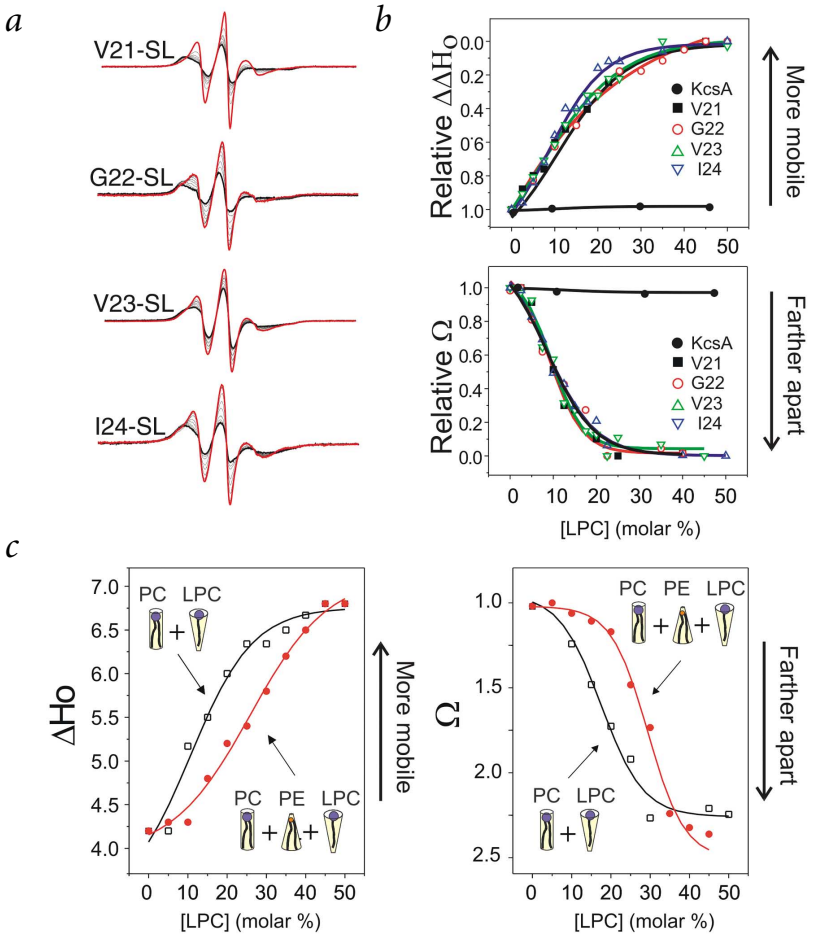

Fig. 5 Mixtures of PC–LPC induce massive conformational changes in MscL ***a***, Room temperature CW-EPR spectra for residues 21–24 obtained at increasing concentrations (molar %) of LPC. Spectral width is 150 G. ***b***, Relative changes in intersubunit proximity (Ω) and spin-label mobility ($\Delta\Delta H_O$, bottom) as a function of LPC molar percent. As in Fig. 2, data were normalized to that in PC18. Dose-response fits to the entire dataset revealed LPC midpoint effects of 9.2 ± 0.9 molar % for changes in Ω, and 11.3 ± 2.3 molar % for changes in ΔH_O. ***c***, Compensatory effects of externally applied 18:1 dioleoyl-phosphatidylethanolamine (PE18) to MscL gating by LPC. Spectral changes are monitored for residue Gly 22-SL as changes in probe mobility (left panel) or in intersubunit proximities (Ω, right panel). Open squares represent data obtained from MscL reconstituted in PC18 (PC + LPC), and filled circles show data in a mixture of PC18–PE18 (60:40 mol:mol). The presence of PE18 shifts the midpoint of LPC activation by 10–15 molar %.

(Ile 24), spin coupling actually returns to values similar to those in the closed state.

Based on these data, we propose that hydrophobic mismatch alone is not enough to drive MscL to its fully open conformation. However, even at the thinnest possible bilayer (PC10), residue Ile 24 still shows evidence of strong spin–spin interactions, implying that this segment of TM1 remains fairly close to the five-fold axis of symmetry. At the same time, several residues (Gly 22, Ile 24, Ile 25 and Ala 27) remain motionally restricted, pointing to limited changes in intersubunit packing relative to the closed state. Indeed, the present results suggest to us that instead of fully opening MscL, a reduction in bilayer thickness might actually stabilize one or more of the several closed states, leading to the fully open state. Although these 'intermediate' closed states might not be detectable electrophysiologically, they can be observed as spectroscopically distinct states. Bilayers formed in PC14 are particularly interesting because they seem to stabilize a structurally distinct closed state with an even narrower permeation path than the closed state in PC18.

Conical lipids stabilize the open state

An alternative approach to modulating the transbilayer lateral tension gradient is through the use of lipid mixtures with different geometries. Previous experiments[23,26] have shown that addition of charged amphiphiles or lysophospholipids to bilayers containing MS channels dramatically lowers the activation threshold in both prokaryotic (MscS) and eukaryotic (TREK-1 and TRAAK) MS channels. In MscL, externally applied lysophosphatidylcholine (LPC) strongly favors the transition to the open state. The addition of LPC (1.5 μM) in the presence of a small transbilayer pressure produces a pronounced increase in MscL single channel activity, even if no additional pressure is applied (Fig. 4*a*). Moreover, once the pressure is released, a large fraction of the channels remain constitutively open, as if LPC incorporation helps liberate some of the membrane lateral tension at rest. Even more remarkably, at larger LPC concentrations (3 μM), MscL activity gradually increases with time in the complete absence of any applied pressure in the pipette (Fig. 4*b*). This behavior mirrors the single channel behavior of MscL at gradually increasing transbilayer pressures and reflects the continuous incorporation or LPC to the external leaflet of the membrane patch (until it breaks).

As above, we monitored LPC-induced conformational rearrangements at the narrowest section of the permeation path (residues 21–24 in TM1, Fig. 1*c*) because these positions were involved in extensive protein–protein contacts and were in close proximity to the five-fold axis of symmetry. Addition of LPC to the liposome suspension produced an increase in the motional freedom of the probe at all positions (Fig. 5*a*). In each case, increasing LPC molar % resulted in spectra that reflected much higher motional freedom with a complete elimination of intersubunit spin–spin interactions, as expected from an opening of the closely packed bundle of TM1 helices. The magnitude of these changes depends on the molar fraction of the added LPC (Fig. 5*a*). Dose-response curves were obtained for residues 21–24 from changes in the mobility parameter (ΔH_O) and the intersubunit proximity parameter (Ω) relative to their values in the closed conformation (no LPC, Fig. 5*b*). In all cases, addition of increasing amounts of LPC produces a decrease in protein–protein contacts, reflecting the apparent separation of the TM segments. The midpoints of the LPC-induced conformational changes, however, are remarkably similar for all of the tested positions. All tested residues had a midpoint of activation near 10 mol %, and no further spectral changes were observed at concentrations beyond 25 mol % LPC by following changes in ΔH_O and Ω. This implies that the individual spectral changes monitor the same global conformational rearrangement in MscL. No effects were detected on probe dynamics or spin–spin interactions if LPC was added to vesicles containing spin-labeled KcsA at different final concentrations (Fig. 5*b*, filled circles).

How are LPC and other 'cone-shaped' lipids able to activate MS channels? In the current hypothesis, the release of intrabilayer lateral pressures is the consequence of shape inequality between bilayer forming (PC) and nonbilayer forming (LPC) lipids (Fig. 1*b*)[23,26]. To directly test this hypothesis, we carried out an experiment using MscL reconstituted into liposomes made from a uniform mixture of PC and phosphatidylethanolamine

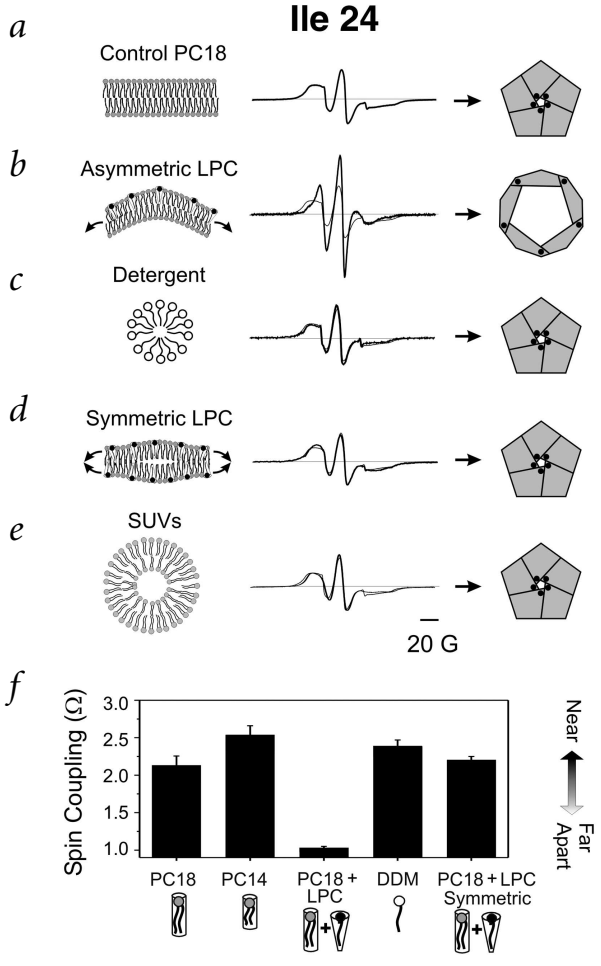

Fig. 6. Asymmetries in the intra-bilayer tension gradient are required for MscL gating. Changes in spectral lineshape from position Ile 24 monitor the influence of different bilayer tension gradients on the conformation of MscL: ***a***, PC18 (closed); ***b***, asymmetric LPC (fully open); ***c***, detergent solution (closed); ***d***, symmetric LPC (closed); and ***e***, small unilamellar vesicles generated by sonication (closed). For the measurements in detergent, Ile 24-SL was resuspended in 0.05% DDM in a solution containing 100 mM $(NH_4)_2SO_4$, 25% triethylene glycol and 3 mM $GdCl_3$, buffered at pH 3.5 with 100 mM glycine[9]. Final protein concentration was ~20 mM. On the left, cartoon diagrams illustrate the different experimental conditions that help manipulate bilayer morphology and mechanical transduction in MscL. The center panels show overlapped CW-EPR spectra of the given experimental condition (thick line) and the spectra in the closed state (thin line). The right panels represent the global conformation of MscL under each experimental condition. ***f***, Analysis of the extent of spin–spin coupling in residue Ile 24-SL under all tested experimental conditions.

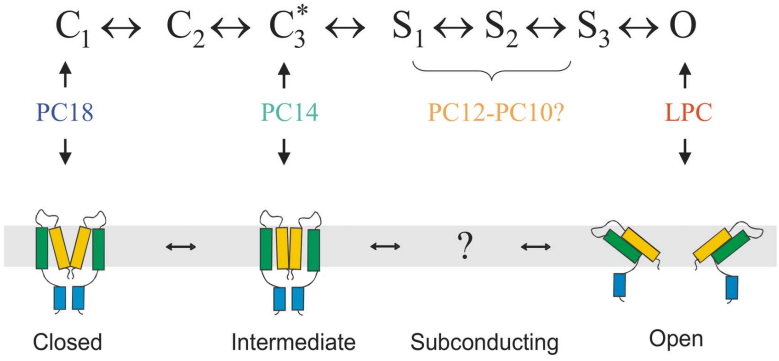

Fig. 7 A model depicting the evolution of structurally distinct conformations during MscL gating. The top row represents a hypothetical sequence of kinetic events MscL undergoes on its way to the fully open state. Manipulating the lipid environment surrounding the channel can trap at least three of these distinct conformations: (i) the closed state is stable in PC18, (ii) PC14 stabilizes a closed conformation further along the kinetic path and (iii) the fully open state can be locked by addition of conical-shaped lipids (LPC) on one leaflet of the bilayer. The possibility remains of stabilizing additional intermediates (such as subconducting states) using even shorter (but more unstable) bilayers.

(PE), and LPC was then added to the extracellular solution. If the shape inequality between PC (a cylindrical bilayer-forming lipid) and LPC (a conical micelle-forming lipid) is at the root of the changes in bilayer lateral pressure, the presence of lipids with shape opposite to that of LPC, such as PE (which is also conical but promotes hexagonal phases), should produce shape complementation. Therefore, they should shift the LPC activation curve towards higher LPC concentrations, assuming that the lipids distribute evenly and do not form separate phases. Our data (Fig. 5*c*) indicate that this is the case. Monitoring MscL conformation at residue Gly 22 in a pure PC18 membrane (open squares), ΔH_O and the Ω parameter show a similar dependence with LPC concentration to those determined with individual residues (Fig. 5*b*; mid point ~13 mol %). However, if the same experiment was repeated for Gly 22 reconstituted in a mixture of 60:40 (mol PC:mol PE, filled circles), the LPC concentration dependence of both structural parameters was shifted ~25 mol %. Again, this effect seems to be a simple shift in intrabilayer pressure without a change in the intrinsic pressure dependence of activation for the channel.

Transbilayer asymmetries and MscL gating

The stabilization of MscL in the open state by LPC–PC mixtures and the opposite role of PE, point towards local shape inequalities as the most probable source of transbilayer pressure distortions that trigger MscL gating. This observation, however, raises an interesting paradox. Because LPC and other conically shaped lipids act as detergents at very high concentrations, open MscL would be expected to be the dominant conformation present in detergent solutions. However, this hypothesis seems to fail when considering that the MscL crystal structure (determined in detergent) corresponds to the closed conformation[9,31]. To solve this apparent inconsistency, we monitored the conformation of MscL from the EPR signal at position Ile 24 in detergent solution and in a series of mixtures of PC and LPC (Fig. 6). In PC18 (Fig. 4*a*), the Ile 24-SL spectrum displays the strong spin–spin interactions characteristic of the closed state. As shown above, addition of LPC to the external leaflet of the bilayer drives MscL into its open conformation (Fig. 6*b*). However, when we recorded the spectra in 0.05% dodecyl maltoside (DDM) using identical conditions as those used for crystallization[9], we were surprised to see that the spectrum was essentially identical to that in PC18 bilayers (Fig. 6*c*), in agreement with the crystallographic data. We interpreted this result to suggest that symmetric lateral pressure changes, such as those generated in a detergent micelle, cannot be transduced by MS channels even though geometric shape inequalities are critical in triggering MscL gating. By extension, symmetrically distributed mixtures of LPC and PC18 would be predicted to fail to open MscL. This is the case; the spectrum of Ile 24-SL MscL reconstituted into preformed LPC–PC18 liposomes (30:70 molar %) is almost indistinguishable from that obtained in PC18 membranes (Fig. 6*d*), as expected from MscL in the closed conformation. Therefore, we propose that the asymmetry in the lateral pressure profile between the two leaflets of the bilayer is what actually initiates the sequence of mechanical transduction steps that leads to the open state. Interestingly, the required degree of asymmetry between the leaflets is larger than initially expected because reconstituting MscL in small sonicated unilamellar vesicles (SUVs), at or near their thermodynamic size limit, fails to open the channels (Fig. 6*e*). Fig. 6*f* shows a comparison of the estimated spin–spin coupling parameter at position Ile 24 for all tested lipid conditions.

Structural snapshots along MscL gating path

By manipulating the nature and extent of lipid–protein interactions, we have been able to stabilize at least two spectroscopically distinct conformations of the large mechanosensitive channel from *E. coli*. We propose that these conformers are structurally equivalent to those populated during the normal evolution of MscL gating under physiological conditions and are represented by the kinetic scheme in Fig. 7. Asymmetric LPC–PC mixtures appear to trap MscL in its fully open conformation, and this trapped state shows similar single channel behavior to that of pressure-activated MscL. Given that the channel does not undergo its gating transition in the presence of symmetrically distributed LPC, it seems unlikely that the observed spectroscopic changes could result from nonspecific subunit dissociation.

PC14 membranes appear to lock an intermediate closed conformation that is characterized by a localized narrowing along the permeation pathway (Fig. 3). This conformation likely follows the fully closed state along the kinetic pathway because it requires smaller external pressures (Fig. 2*a*; Table 1) to transition to the fully open state (Fig. 7). Nevertheless, this intermediate state might not be kinetically connected to the LPC-stabilized open state, representing instead a separate kinetic and structural path. Additional characterization is necessary to establish the functional nature of the structural intermediates stabilized in PC12 and PC10, because standard patch-clamp methods do not seem to be the method of choice for thin bilayers. However, because MscL is known to populate a series of subconducting states before reaching the open conformation[36], it is easy to speculate that these intermediates might represent some of these subconducting states. The remarkable stability of the open conformation in asymmetrically distributed mixtures of PC–LPC will not only help establish the nature of the deformations in the transbilayer pressure profile capable of triggering MscL opening,

but it has clearly set the stage for a detailed structural analysis of its gating mechanism.

Methods

Mutant production, expression and purification. Cys mutants were generated by oligonucleotide mismatch site-directed mutagenesis using the Transformer kit (Clonetec) as described[31] and confirmed by dideoxy DNA sequencing. Mutant channels were expressed and purified as reported[31] except for the use of M15 as the *E. coli* strain. Briefly, the construct MscL-pQE32 containing MscL with the RGS-His_4 epitope at the N-terminus was used to transform *E. coli* M15 cells (Clontech) using standard chemical methods. Membranes were solubilized in PBS containing dodecyl maltoside (DDM) at room temperature, spun down at 100,000*g* for 1 h and purified with a Co^{2+}-based metal-chelate chromatography resin (Talon resin, Clontech).

Reconstitution into lipid vesicles. MscL was reconstituted into artificial liposomes for patch-clamp experiments as described[37–39]. Small aliquots of asolectin (containing the carbon chains C16:0, C18:0, C18:2 and C18:3, of which C18:2 comprised 60%), PC16, PC18 or PC20 dissolved in chloroform were dried under nitrogen; resuspended in 2.5 mM HEPES, pH 7.2, and 150 mM KCl; and bath-sonicated for 4 min. Purified MscL protein was added at the desired protein:lipid ratio and then mixed with BioBeads (BioRad) for 3 h at room temperature. Liposomes were collected by ultracentrifugation at 90,000*g* for 30 min at 4 °C and resuspended in dehydration/rehydration (D/R) buffer (5 mM HEPES, pH 7.2, and 200 mM KCl).

Liposome patch clamp. Aliquots of the liposomes were spotted onto glass slides and allowed to dehydrate for 4–6 h followed by overnight rehydration in D/R buffer under humid conditions. Currents from isolated liposome patches were recorded using standard patch clamp in a solution containing 200 mM KCl, 40 mM $MgCl_2$ and 5 mM HEPES-KOH, pH 7.2. Transbilayer pressure differences were established by application of suction to the patch-clamp pipette and measured by a piezoelectric pressure transducer (Omega). Single channel currents were filtered at 1 kHz and digitized at 5 kHz.

Spin labeling and EPR spectroscopy. For EPR spectroscopy, the purified mutant MscL was spin labeled twice for 1 h with methanethiosulfonate spin label (Toronto Research) at a 10:1 label:channel molar ratio. Labeling was done in detergent solution at room temperature. After eliminating unreacted label by gel filtration chromatography, channels were concentrated, reconstituted at a 500:1 lipid:channel molar ratio by dilution in PBS and collected by centrifugation. EPR spectroscopy was performed as described[31,40]. X-band Continuous Wave (CW) EPR spectra were obtained in a Bruker EMX spectrometer fitted with a loop-gap resonator under the following conditions: 2 mW incident power, 100 kHz modulation frequency and 1 G modulation amplitude. All spectra were obtained at room temperature.

Conformational changes in MscL were detected by following the dynamic behavior of the spin label and the relative broadening resulting from closed proximity to neighboring subunits. Probe dynamics (mobility) was obtained from an empiric analysis of the EPR lineshape, reflecting the degree of motional restriction of the nitroxide spin label. This was quantified as the width of the central resonance line ΔH_O or the difference in central resonance width from two different conditions ($\Delta\Delta H_O$)[41,42]. Changes in intersubunit proximity were derived from spectral broadenings derived from the intersubunit spin–spin interactions. Unfortunately, because MscL is a homopentamer with five-fold symmetry, actual distances cannot be easily computed. Instead, a rough estimate of intersubunit proximities was obtained from a qualitative analysis of electron spin–spin interactions using the Ω parameter[43]. This is derived from the ratio of normalized spectral amplitudes of a fully labeled sample relative to one with no spin–spin interactions (typically underlabeled at a 1:10 ratio).

EPR experiments at increasing LPC concentrations were carried out from a single stock of reconstituted, spin-labeled MscL. This stock was divided into 10 identical aliquots and LPC was added at specific lipid:lipid molar % at a constant final volume.

Effects of LPC on membrane structure and dynamics. Three control experiments were carried out to demonstrate that LPC activation of MscL is not the result of nonspecific detergent-like effects or the removal of the bilayer. (i) Electron microscopy and (ii) light scattering experiments confirmed that although liposome size decreased with a half LPC concentration near 12 mol %, they remained vesiculated even at the highest LPC:PC ratios. (iii) EPR measurements revealed that the motional dynamics of spin-labeled phospholipids (5-deoxy-phosphatidylcholine and glycero-3-phospho-TEMPO-choline) is unaffected at all tested LPC:PC ratios.

Acknowledgments

We thank T. Thompsom and R. Biltonen for insightful discussions and C. Ptak for critically reading the manuscript. Support and encouragement from S. Mochel is greatly appreciated. This work was supported in part by NIH (E.P.) and the McKnight endowment fund for neuroscience (E.P.), the Australian Research Council (B.M.) and the Australian Academy of Science (Scientific Visit Award to B.M).

Competing interests statement

The authors declare that they have no competing financial interests.

Received 28 March, 2002; accepted 2 July, 2002.

1. Sukharev, S.I., Blount, P., Martinac, B. & Kung, C. Mechanosensitive channels of *Escherichia coli*: the MscL gene, protein, and activities. *Annu. Rev. Physiol.* **59**, 633–657 (1997).
2. Booth, I.R. & Louis, P. Managing hypoosmotic stress: aquaporins and mechanosensitive channels in *Escherichia coli*. *Curr. Opin. Microbiol.* **2**, 166–169 (1999).
3. Wood, J.M. Osmosensing by bacteria: signals and membrane-based sensors. *Microbiol. Mol. Biol. Rev.* **63**, 230–262 (1999).
4. Hamill, O.P. & Martinac, B. Molecular basis of mechanotransduction in living cells. *Physiol. Rev.* **81**, 685–740 (2001).
5. Martinac, B. Mechanosensitive channels in prokaryotes. *Cell. Physiol. Biochem.* **11**, 61–76 (2001).
6. Martinac, B., Buechner, M., Delcour, A.H., Adler, J. & Kung, C. Pressure-sensitive ion channel in *Escherichia coli*. *Proc. Natl. Acad. Sci. USA* **84**, 2297–2301 (1987).
7. Sukharev, S.I., Martinac, B., Arshavsky, V.Y. & Kung, C. Two types of mechanosensitive channels in the *Escherichia coli* cell envelope: solubilization and functional reconstitution. *Biophys. J.* **65**, 177–183 (1993).
8. Sukharev, S.I., Blount, P., Martinac, B., Blattner, F.R. & Kung, C. A large-conductance mechanosensitive channel in *E. coli* encoded by MscL alone. *Nature* **368**, 265–268 (1994).
9. Chang, G., Spencer, R.H., Lee, A.T., Barclay, M.T. & Rees, D.C. Structure of the MscL homolog from *Mycobacterium tuberculosis*: a gated mechanosensitive ion channel. *Science* **282**, 2220–2226 (1998).
10. Berrier, C., Coulombe, A., Houssin, C. & Ghazi, A. A patch-clamp study of ion channels of inner and outer membranes and of contact zones of *E. coli*, fused into giant liposomes. Pressure-activated channels are localized in the inner membrane. *FEBS Lett.* **259**, 27–32 (1989).
11. Cantor, R.S. Lateral pressures in cell membranes: a mechanism for modulation of protein function. *J. Phys. Chem. B* **101**, 1723–1725 (1997).
12. Cantor, R.S. Lipid composition and the lateral pressure profile in bilayers. *Biophys J.* **76**, 2625–2639 (1999).
13. Mouritsen, O.G. & Bloom, M. Mattress model of lipid-protein interactions in membranes. *Biophys. J.* **46**, 141–153 (1984).
14. Gruner, S. in *Biologically Inspired Physics* (ed. Peliti, L.) 127–135 (Plenum, New York; 1991).
15. Israelachvili, J. *Intermolecular and Surface Forces* (Academic Press, New York; 1992).
16. Killian, J.A. Hydrophobic mismatch between proteins and lipids in membranes. *Biochim. Biophys. Acta* **1376**, 401–415 (1998).
17. Cornea, R.L. & Thomas, D.D. Effects of membrane thickness on the molecular dynamics and enzymatic activity of reconstituted Ca-ATPase. *Biochemistry* **33**, 2912–2920 (1994).
18. Galbraith, T.P. & Wallace, B.A. Phospholipid chain length alters the equilibrium between pore and channel forms of gramicidin. *Faraday Discuss.* **111**, 159–164 (1998).
19. Lundbaek, J.A. & Andersen, O.S. Spring constants for channel-induced lipid bilayer deformations. Estimates using gramicidin channels. *Biophys. J.* **76**, 889–895 (1999).
20. Dumas, F., Tocanne, J.F., Leblanc, G. & Lebrun, M.C. Consequences of hydrophobic mismatch between lipids and melibiose permease on melibiose transport. *Biochemistry* **39**, 4846–4854 (2000).
21. Lewis, B.A. & Engelman, D.M. Lipid bilayer thickness varies linearly with acyl chain length in fluid phosphatidylcholine vesicles. *J. Mol. Biol.* **166**, 211–217 (1983).
22. Gruner, S.M. Intrinsic curvature hypothesis for biomembrane lipid composition: a role for nonbilayer lipids. *Proc. Natl. Acad. Sci. USA* **82**, 3665–3669 (1985).
23. Martinac, B., Adler, J. & Kung, C. Mechanosensitive ion channels of *E. coli* activated by amphipaths. *Nature* **348**, 261–263 (1990).
24. Lundbaek, J.A. & Andersen, O.S. Lysophospholipids modulate channel function by altering the mechanical properties of lipid bilayers. *J. Gen. Physiol.* **104**, 645–673 (1994).
25. Casado, M. & Ascher, P. Opposite modulation of NMDA receptors by lysophospholipids and arachidonic acid: common features with mechanosensitivity. *J. Physiol.* **513**, 317–330 (1998).
26. Maingret, F., Patel, A.J., Lesage, F., Lazdunski, M. & Honoré, E. Lysophospholipids open the two-pore domain mechano-gated K^+ channels TREK-1 and TRAAK. *J. Biol. Chem.* **275**, 10128–10133 (2000).
27. Mandersloot, J.G., Reman, F.C., Van Deenen, L.L. & De Gier, J. Barrier properties of lecithin/lysolecithin mixtures. *Biochim. Biophys. Acta* **382**, 22–26 (1975).
28. Hubbell, W.L., Gross, A., Langen, R. & Lietzow, M.A. Recent advances in site-directed spin labeling of proteins. *Curr. Opin. Struct. Biol.* **8**, 649–656 (1998).
29. Hubbell, W.L., Cafiso, D.S. & Altenbach, C. Identifying conformational changes with site-directed spin labeling. *Nature Struct. Biol.* **7**, 735–739 (2000).
30. Mchaourab, H. & Perozo, E. in *Biological Magnetic Resonance* Vol. 19 (ed. S. Eaton, G.E. & Berliner, L.) 155–218 (Kluwer-Plenum, New York; 2000).
31. Perozo, E., Kloda, A., Cortes, D.M. & Martinac, B. Site-directed spin-labeling analysis of reconstituted MscL in the closed state. *J. Gen. Physiol.* **118**, 193–206 (2001).
32. Ou, X., Blount, P., Hoffman, R.J. & Kung, C. One face of a transmembrane helix is crucial in mechanosensitive channel gating. *Proc. Natl. Acad. Sci. USA* **95**, 11471–11475 (1998).
33. Sukharev, S., Betanzos, M., Chiang, C.-S. & Guy, H.R. The gating mechanism of the large mechanosensitive channel MscL. *Nature* **409**, 720–724 (2001).
34. Sukharev, S., Durell, S.R. & Guy, H.R. Structural models of the MscL gating mechanism. *Biophys. J.* **81**, 917–936 (2001).
35. Gullingsrud, J., Kosztin, D. & Schulten, K. Structural determinants of MscL gating studied by molecular dynamics simulations. *Biophys. J.* **80**, 2074–2081 (2001).
36. Sukharev, S.I., Sigurdson, W.J., Kung, C. & Sachs, F. Energetic and spatial parameters for gating of the bacterial large conductance mechanosensitive channel, MscL. *J. Gen. Physiol.* **113**, 525–540 (1999).
37. Delcour, A.H., Martinac, B., Adler, J. & Kung, C. Modified reconstitution method used in patch-clamp studies of *Escherichia coli* ion channels. *Biophys. J.* **56**, 631–636 (1989).
38. Häse, C.C., Le Dain, A.C. & Martinac, B. Purification and functional reconstitution of the recombinant large mechanosensitive ion channel (MscL) of *Escherichia coli*. *J. Biol. Chem.* **270**, 18329–18334 (1995).
39. Cruickshank, C.C., Minchin, R.F., Le Dain, A.C. & Martinac, B. Estimation of the pore size of the large-conductance mechanosensitive ion channel of *Escherichia coli*. *Biophys. J.* **73**, 1925–1931 (1997).
40. Cortes, D.M., Cuello, L.G. & Perozo, E. Molecular architecture of full-length KcsA: role of cytoplasmic domains in ion permeation and activation gating. *J. Gen. Physiol.* **117**, 165–180 (2001).
41. Mchaourab, H.S., Lietzow, M.A., Hideg, K. & Hubbell, W.L. Motion of spin-labeled side chains in T4 lysozyme. Correlation with protein structure and dynamics. *Biochemistry* **35**, 7692–7704 (1996).
42. Columbus, L., Kálai, T., Jekö, J., Hideg, K. & Hubbell, W.L. Molecular motion of spin labeled side chains in α-helices: analysis by variation of side chain structure. *Biochemistry* **40**, 3828–3846 (2001).
43. Perozo, E., Cortes, D.M. & Cuello, L.G. Three-dimensional architecture and gating mechanism of a K^+ channel studied by EPR spectroscopy. *Nature Struct. Biol.* **5**, 459–469 (1998).